Programmed cell death during *Drosophila* embryogenesis

John M. Abrams[1], Kristin White[1], Liselotte I. Fessler[2] and Hermann Steller[1]

[1]Howard Hughes Medical Institute, Department of Brain and Cognitive Sciences and Department of Biology, Massachusetts Institute of Technology, Cambridge, Massachusetts 02139, USA
[2]Molecular Biology Institute and Biology Department, University of California, Los Angeles, CA 90024, USA

SUMMARY

The deliberate and orderly removal of cells by programmed cell death is a common phenomenon during the development of metazoan animals. We have examined the distribution and ultrastructural appearance of cell deaths that occur during embryogenesis in *Drosophila melanogaster*. A large number of cells die during embryonic development in *Drosophila*. These cells display ultrastructural features that resemble apoptosis observed in vertebrate systems, including nuclear condensation, fragmentation and engulfment by macrophages. Programmed cell deaths can be rapidly and reliably visualized in living wild-type and mutant *Drosophila* embryos using the vital dyes acridine orange or nile blue. Acridine orange appears to selectively stain apoptotic forms of death in these preparations, since cells undergoing necrotic deaths were not significantly labelled. Likewise, toluidine blue staining of fixed tissues resulted in highly specific labelling of apoptotic cells, indicating that apoptosis leads to specific biochemical changes responsible for the selective affinity to these dyes. Cell death begins at stage 11 (~7 hours) of embryogenesis and thereafter becomes widespread, affecting many different tissues and regions of the embryo. Although the distribution of dying cells changes drastically over time, the overall pattern of cell death is highly reproducible for any given developmental stage. Detailed analysis of cell death in the central nervous system of stage 16 embryos (13-16 hours) revealed asymmetries in the exact number and position of dying cells on either side of the midline, suggesting that the decision to die may not be strictly predetermined at this stage. This work provides the basis for further molecular genetic studies on the control and execution of programmed cell death in *Drosophila*.

Key words: apoptosis, *Drosophila*; embryogenesis, programmed cell death, vital dyes, nervous system development, macrophages

INTRODUCTION

Cell death is a ubiquitous feature of metazoan development (see for example Wyllie et al., 1980; Bowen and Lockshin, 1981; Truman, 1984; Ellis et al., 1991; Tomei and Cope, 1991; Raff, 1992). Studies from a broad range of vertebrate and invertebrate systems have established that such naturally occurring cell death results from an active developmental program often triggered by systemic hormones, withdrawal of trophic factors and local cell interactions (Saunders, 1966; Truman, 1984; Oppenheim, 1985). In many animal systems, this deliberate removal of cells proceeds through a series of distinct morphological stages known as apoptosis (Kerr et al., 1972; Wyllie et al., 1980). During apoptotic death, the cytoplasm and nucleus of the dying cell condense while the morphology of cellular organelles remains rather well preserved. In many cases, the condensing cell breaks up into fragments (apoptotic bodies) and is eventually engulfed by phagocytic cells. The regional incidence of cell death during development is often predictable (Whitten, 1969; Hinchcliffe, 1981; Hurle, 1988) and, at least in some cases, depends on protein synthesis (Tata, 1966; Lockshin, 1969; Farbach and Truman, 1988;

Martin et al., 1988; Oppenheim et al., 1990). Genetic studies of cell death in *C. elegans* have identified several loci that are required for this process during development (Ellis and Horvitz 1986; Yuan and Horvitz, 1990; Ellis et al., 1991; Hengartner et al., 1992). These and other observations have led to the concept of 'programmed cell death', which views cell loss as the consequence of an active physiological process analogous, in some ways, to differentiation (Saunders, 1966; Lockshin and Zakeri, 1991; Raff, 1992). Although the extrinsic signals that elicit programmed cell death have been characterized in some cases, the exact molecular mechanisms underlying programmed cell death remain unknown.

We are interested in a molecular genetic analysis of cell death in *Drosophila*. Several examples of naturally occurring cell death during postembryonic development have been documented in this organism. In these cases, the decision to die can require hormone induction (Truman, 1984; Kimura and Truman, 1990) and may be influenced by cell interactions (Fischbach and Technau, 1984; Wolff and Ready, 1991; Campos et al., 1992). In contrast, little is known about programmed cell death in the *Drosophila* embryo (Campos-Ortega and Hartenstein, 1985).

Since we felt that the *Drosophila* embryo would be particularly amenable to future genetic and molecular analyses of programmed cell death, we have investigated the morphology and distribution of cell deaths that normally occur during embryonic development. We find that a large number of cells undergo programmed death, and that these cells display many of the characteristic ultrastructural features described for apoptosis in other organisms. Apoptotic cells can be rapidly and reliably visualized in live embryos with vital dyes. We demonstrate that at least one of these stains, acridine orange, is specific for apoptotic forms of cell death and does not significantly label cells undergoing necrotic death provoked by injury. Although the number and location of apoptotic cells changes dramatically over the course of embryogenesis, we find that the overall pattern of cell death is reproducible for any given developmental stage. However, close examination of certain regions, particularly in the developing central nervous system, indicates that the exact number and position of apoptotic cells can vary. These observations suggest that the decision to die is not strictly stereotyped for all cells in the embryo and may be influenced by local intercellular interactions. Finally, this work has provided the basis for the isolation of cell death defective mutations in *Drosophila* (White, K., Abrams, J. M., Grether, M., Young, L. and Steller, H. unpublished data).

MATERIALS AND METHODS

Egg collection and embryo staging

Wild-type (Canton S) eggs were collected on molasses/agar plates, either at 25°C or at 18°C, and staged according to Campos-Ortega and Hartenstein (1985). Tightly staged populations of embryos were prepared by sorting blastoderms on the basis of their characteristic morphology. Where appropriate, age is stated as time after egg laying (AEL). Embryos from stocks of *polyhomeotic* [505] (Dura et al., 1987) and *crumbs*[11A22] (Tepass et al., 1990) were also analyzed.

Staining with vital dyes

Embryos were dechorionated with 50% bleach, rinsed with water and placed in an equal volume of heptane and either 5 μg/ml of acridine orange (Sigma) or 100 μg/ml nile blue A (Sigma) in 0.1 M phosphate buffer, pH ~ 7.2. After 5 minutes of shaking, embryos were removed from the interface and placed under series 700 Halocarbon oil, (Halocarbon products corp., Hackensack, NJ). Samples were viewed either with a conventional fluorescence microscope or with an MRC 600 confocal scanning laser microscope (Bio-Rad) using a BHS color cube filter to detect green fluorescence or a YHS color cube filter to detect red fluorescence. Confocal image processing was performed either with software provided by the manufacturer or with the Voxel View (Vital Images, Iowa) program on a Silicon Graphics computer. Acridine-stained embryos can be viewed with filters for either green or red fluorescence and, in general, these patterns are similar. Photographic representations shown here have been viewed using the green filter unless otherwise noted. For time-lapse studies, acridine-stained embryos were placed under Voltalef oil (3 s or 10 s) on Petri-perm dishes (Bachofer, Reutlingen, Germany).

Fixed tissue spreads

Embryos were stained with acridine orange as described above,

washed in phosphate buffer to remove heptane, and individually placed on slides coated with 0.5% gelatin and 0.05% chrom alum. A siliconized cover slip placed over the embryo was used to gently spread the tissue into a monolayer. After photographic recordings of representative fields, the slides were rapidly frozen at –70°C. To fix the tissue, the cover slip was quickly removed and slides were immediately submerged in 2.5% glutaraldehyde for 20 minutes. For toluidine blue staining, glutaraldehyde-fixed tissue was placed in 1% osmium tetroxide for 5 minutes, washed with water, air dried and then stained with a solution of 0.1% toluidine/0.1% sodium borate for 5 minutes at 55°C.

Electron microscopy

Dechorionated embryos were shaken in equal volumes of heptane and a fixative solution of 1.5% acrolein, 1% paraformaldehyde, 2% glutaraldehyde in 0.1 M phosphate buffer, pH 7.0, for 20 minutes. Embryos were then freed of the surrounding vitelline membranes by hand dissection in 0.1 M phosphate buffer, pH 7.0, (PB) and refixed for another 30 minutes in the above fixative solution. After several washes in PB, the embryos were treated with a 2% solution of osmium tetroxide in PB for 1 hour. Following several washes in PB, the embryos were dehydrated through an ethanol series, washed in several changes of propylene oxide and then embedded in Spurr's media (Polysciences, Warrington, PA; Spurr, 1969). Thin sections were stained with uranyl aceytate and lead citrate according to Osborne (1980). Alternatively, after osmium fixation, some embryos were washed in water and incubated in 1% uranyl acetate (in water) at 50°C for 12-16 hours. Thin sections from these samples were viewed directly by electron microscopy without any subsequent staining. For light microscopy, sections were stained with 0.01% toluidine/0.05% sodium borate with or without 0.05% methylene blue at 55°C for approximately 5 minutes.

Irradiation of embryos and cycloheximide treatment

3-4 hours after egg laying (AEL), Canton S embryos were exposed to 600 or 4000 rads of X-irradiation using a Torrex 120D X-ray inspection system (Astrophysics Research Corp., CA). Compared to a hatching frequency ≥90% for untreated embryos, these protocols of X-irradiation reduced the hatching frequency to ~ 5% for a 600 rad exposure or 0% for a 4000 rad exposure. Some embryos irradiated at 4000 rads were treated with cycloheximide immediately afterward, by shaking them in heptane and 10 μg/ml cycloheximide (in 0.1 M phosphate buffer). These embryos, along with mock-treated samples, were aged for various times under Voltalef oil.

Hypoxia treatments

10-12 hours AEL embryos were dechorinonated and placed under heptane for 4 hours at 25°C. Survival after this treatment is 0% (no hatched embryos observed out of 400 scored). Embryos subjected to this treatment were either stained with vital dyes or prepared for electron microscopy.

Antibody staining

Phagocytic hemocytes are detected with a rat polyclonal antibody to protein X. Protein X is one of the abundant secreted proteins found in the medium of Kc cell cultures (Echalier, 1976). This protein has been purified by previously described techniques (Olson et al., 1990). Anti-X polyclonal antibodies were raised in a rat using pure, nonreduced protein X as immunogen. For some whole-mount preparations, a 1:500 dilution of this antiserum was used and immunostaining with HRP-conjugated secondary antibody was performed essentially as described in Steller et al. (1987) except that post-fixation washes and blocking steps were done as

described in Lee et al. (1991). Embryos prepared for subsequent histology were immunostained with anti-X, biotinylated anti-rat-IgG and avidin-peroxidase using the ABC Vectastain kit (Vector Labs, Burlingame, CA). After color development, the embryos were dehydrated, embedded in Epon (Polysciences, Warrington, PA) and sectioned. The sections were then stained with 0.01% toluidine Blue, 0.025% methylene blue in 0.025% sodium tetraborate at 70-77°C.

RESULTS

Cell death in the *Drosophila* embryo occurs by apoptosis

Comparative studies from a wide variety of organisms have defined a set of strikingly conserved morphological features associated with the regulated death of cells during development (Kerr et al., 1972; Wyllie et al., 1980). This type of death, conventionally referred to as apoptosis or programmed cell death, involves a generalized condensation of the cytoplasm and nucleus, separation of the dying cell from its neighbors, fragmentation into discrete membrane-bound

bodies and eventual engulfment of cellular debris and corpses by phagocytes (Kerr et al., 1972; Wyllie et al., 1980). A characteristic feature of apoptotic death is that, in spite of these cytologic changes, organelles remain intact and are often identifiable even after engulfment (Kerr and Harmon, 1991). In contrast, a distinctly different set of ultrastructural features is typically observed under conditions that induce cellular injury or necrosis (Wyllie, 1981; Kerr and Harmon, 1991). This form of death includes a general swelling of the cell and its organelles, loss of membrane integrity, lysosomal rupture and ultimate disintegration of organelles (for example see Trump et al., 1981; Wyllie, 1981; see also Fig. 7). We wanted to determine whether the ultrastructural morphology of embryonic cell death in *Drosophila* resembles the apoptotic cell deaths previously observed in other systems. Fig. 1 is a compilation of various stages of cellular degeneration from electron microscopic images of a stage 13 embryo. At this point during embryogenesis, cell death is prominent and widespread. The resemblance of these degenerating bodies to the apoptotic figures that have been described in other
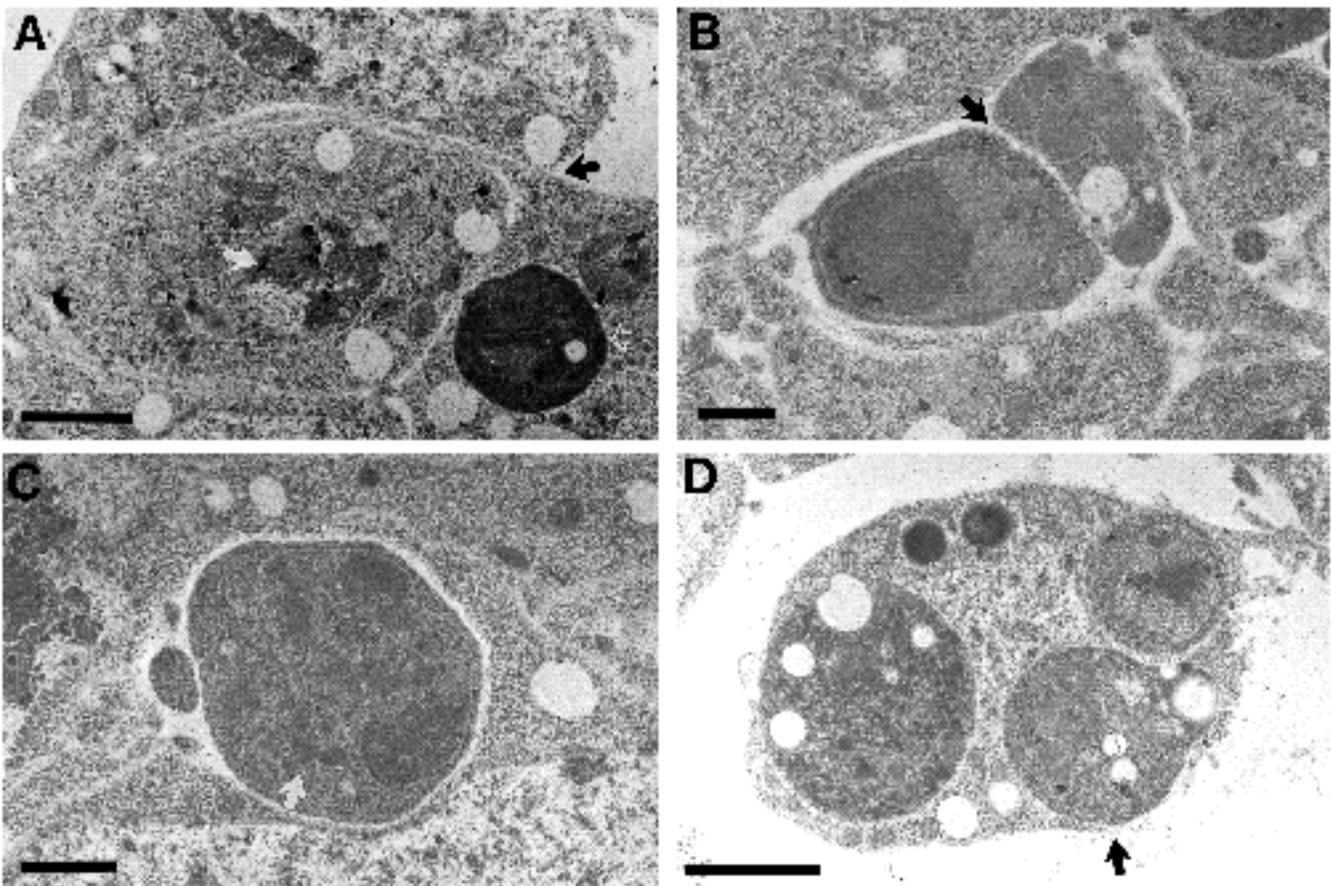

Fig. 1. Electron micrographs of cell death in a stage 13 wild-type embryo. (A) Early stage of cell death in the epidermal layer. The dying cell has begun to separate from its neighbors and masses of compacted nuclear material are apparent (white arrow) yet mitochondria appear normal. A macrophage, already containing one apoptotic corpse (open white arrow), is extending a phagocytic pseudopodium (black arrow) around the dying cell which is already an apparent target for engulfment; scale bar, 2.4 µm. (B) A fragmenting cell corpse is fully separated from neighboring cells. Cytoplasmic bridges (black arrow) still join the separating fragments; scale bar, 1 µm. (C) Fragmented cell corpse. Cytoplasm is condensed yet mitochondria (arrow) are still recognizable; scale bar, 1 µm. (D) Macrophage engorged with cell corpses, one of which (arrow) contains readily identifiable mitochondria; scale bar, 2 µm.

animal systems is striking. Early signs of programmed cell death are depicted in Fig. 1A, where compaction of chromatin into electron-dense masses and cellular shrinkage have become apparent. The mitochondria are clearly identifiable and apparently unaffected at this stage of cell death. As degeneration progresses, dying cells separate from their neighbors, becoming further condensed and osmiophilic. At this stage, fragmentation into membrane-bound bodies often ensues (see Fig. 1B). While nuclear components become highly compacted, the condensing cytoplasm frequently contains intact mitochondria (Fig. 1C). Dying cells and corpses can exist as free, unengulfed material or, more often, they are observed inside large phagocytes that may contain several degenerate bodies (see Fig. 1D and below). From our analyses, it appears that the engulfment of cell corpses during embryogenesis occurs mostly, if not exclusively, by circulating macrophage-like cells (see below).

The stage at which a dying cell becomes a target for engulfment is apparently quite variable. Late-stage apoptotic bodies, which have deteriorated to the extent that organelles are no longer identifiable, are frequently being engulfed by macrophages (not shown). Some dying cells that have been entirely phagocytosed, however, contain identifiable mitochondria and other organelles characteristic of earlier stages of degeneration (see Fig. 1D). We have also observed macrophages approaching cells showing only very early signs of death. For example, in Fig. 1A, a cell in a very early stage of apoptosis (its nucleus is only par-

tially osmophilic) is in close contact with an engulfing macrophage. Thus, while many dying cells are engulfed at a fairly late stage of degeneration, when the entire cell is fully condensed, there are also instances of early engulfment prior to complete nuclear condensation.

From our ultrastructural analyses, it is clear that the vast majority of natural cell deaths in the *Drosophila* embryo occur by apoptosis. These structural features contrast starkly with the cytologic changes observed when embryonic cells undergo necrosis (see Fig. 7).

Degenerating cells in fixed tissue preparations are readily identified with histological stains (Bowen, 1981, Fischbach and Technau, 1984), including toluidine blue (Fristrom, 1969; Murphy, 1974; Giorgi and Deri, 1976). However, these studies made no clear distinction between apoptotic and necrotic forms of death. To examine the correspondence between the above ultrastructural observations with light microscopy, we stained semithin plastic sections with toluidine blue, and examined adjacent ultrathin sections in the electron microscope (Fig. 2). In this way, we were able to compare the ultrastructure and staining properties of the same cell. In the light microscope, dying cells are distinguished as condensed figures which become heavily stained with toluidine blue (Fig. 2C,D). Ultrastructural examination of the same region revealed that the intensely stained (chromophilic) cells displayed obvious apoptotic features (Fig. 2, compare A,C with B,D). Note that only the apoptotic corpses, but not the cytoplasm of the engulf-
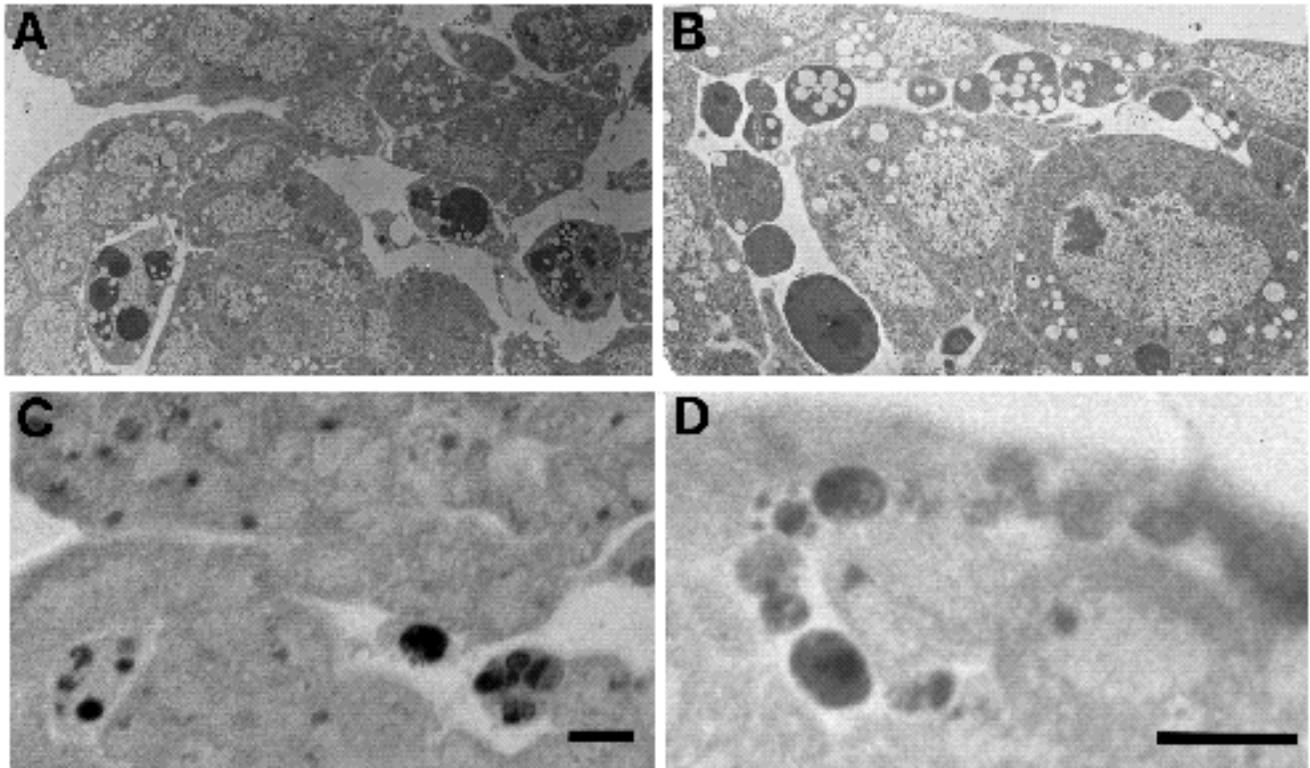

Fig. 2. Apoptotic cells are stained by toluidine blue. (A) Electron micrograph of phagocytic macrophages containing apoptotic cell corpses and (C) the same region of tissue in a neighboring toluidine-blue-stained semithin section seen by Nomarski optics. (B) Electron micrograph of unengulfed apoptotic bodies and (D) the same region of tissue in a neighboring toluidine-blue-stained semithin section seen by Nomarski optics. Images are from a stage 13 embryo. Scale bars, 5 µm.
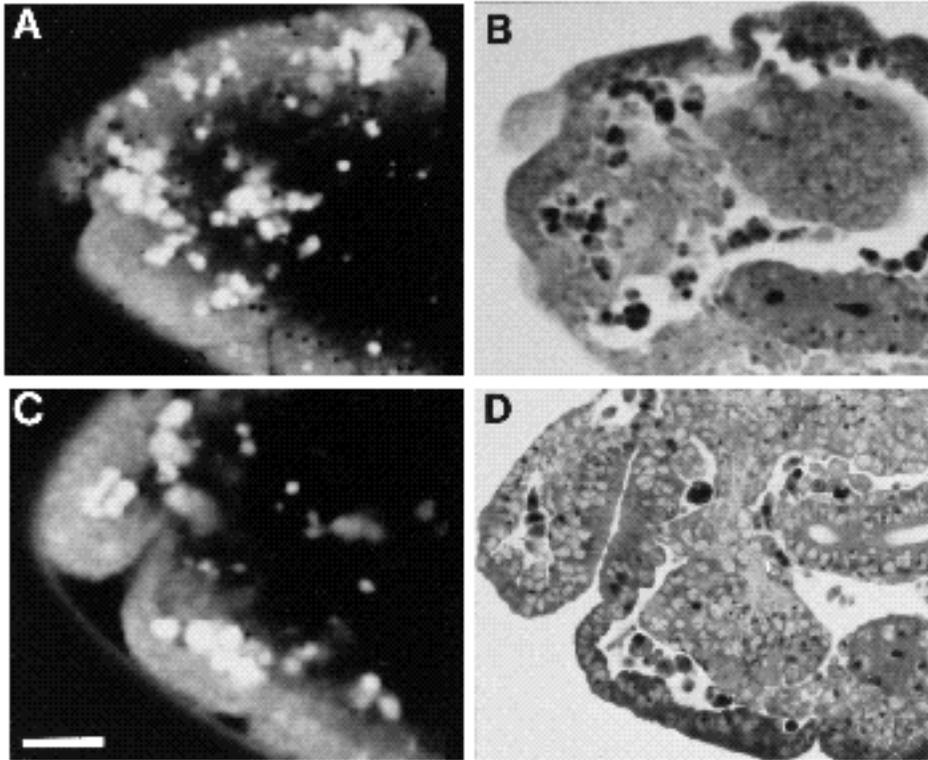
Fig. 3. AO-stained cells in vivo correspond to the position of pyknotic cells in fixed tissue. (A,C) Confocal optical sections from head region of AO-stained embryos and (B,D) toluidine-stained plastic sections from the head region of stage 13/14 embryos. At this stage of head development, intensely stained cells are observed in the clypeolabrum and in the subepidermal spaces associated with the the maxillary bud, the dorsal ridge and the brain. A and B are comparable sections as are C and D. Anterior is to the left, dorsal is up. Note that the in vivo distribution of brightly stained AO-positive cells is similar to the distribution of dark, pyknotic figures in plastic sections. Scale bar, 20 µm.

ing phagocytes, are stained by toluidine blue (for example see Fig. 2C). These results show that toluidine blue is a reliable stain for apoptotic cells in the *Drosophila* embryo. Furthermore, it generally appears that ultrastructural changes associated with cell death precede the changes that cause dying cells to become characteristically chromophilic (data not shown). Also, as we show below, this increased chromophilic property appears to be specific for apoptotic forms of cell death, since necrotic cells remain unstained.

Identification of apoptotic cells in live embryos
In order to investigate the pattern of programmed cell death throughout embryonic development, and as a prerequisite for genetic screens, we sought rapid and reliable methods to visualize apoptotic cells in the *Drosophila* embryo. Vital dyes have been previously used to investigate cell death in a variety of developmental preparations (Saunders et al., 1962; Robbins and Marcus, 1963; Spreij, 1971; Starre-van der Molen and Otten, 1974; Wolff and Ready, 1991; Bonini et al., 1990). Based on these methods, we developed a simple protocol for staining apoptotic cells in live *Drosophila* embryos (see Materials and Methods). Using heptane permeabilization, live embryos were stained with the vital dyes acridine orange (AO) or nile blue (NB) and then viewed by conventional or confocal microscopy. With confocal microscopy and time-lapse imaging, we can usually follow these AO-positive cells for at least 30 minutes (not shown). The patterns of staining obtained in this fashion were found to closely resemble the distribution of pyknotic figures in toluidine-blue-stained plastic sections. Fig. 3 compares optical sections obtained by confocal microscopy from the head region of an AO-stained embryo (stage 13) with toluidine-blue-stained plastic sections from

equivalent sagittal planes of a comparably staged embryo. There is an excellent correspondence between the position of brightly fluorescent cells in whole-mount embryos and the distribution of darkly stained degenerating figures in plastic sections. Embryos stained with another vital dye, nile blue (NB), display patterns which are identical to those seen with AO (not shown). Furthermore, simultaneous co-staining with these two dyes shows a precise correspondence between AO-positive figures and NB-positive figures (not shown).

Previous studies (Saunders, 1962; Spreij, 1971) did not resolve whether vital dyes label dying cells per se, or whether they merely provide an indicator of cellular activity associated with degeneration, such as phagocytosis (for example see Savill et al., 1990 and below). Therefore, to achieve higher resolution of the structures that stain with vital dyes and compare them to those that stain with toluidine blue after fixation, we analyzed tissue spreads of embryonic material. Because specific staining with these vital dyes is compromised after fixation, our analyses were performed in sequential fashion. Embryos were first stained in vivo with AO and then spread onto coated glass slides to dissociate the tissue (see Methods). After photographically recording representative fields of tissue under fluorescence microscopy, these preparations were then fixed and stained with toluidine blue using standard histological procedures (see methods). In this fashion, the cytology of previously identified AO-positive cells could then be reassessed by returning to the exact same field of tissue (see Methods). The vast majority of toluidine-blue-positive cells (Fig. 4B) were clearly positive for AO fluorescence (Fig. 4A). We also observed a few cells that stained for either AO or toluidine blue but failed to stain for both. Reasons
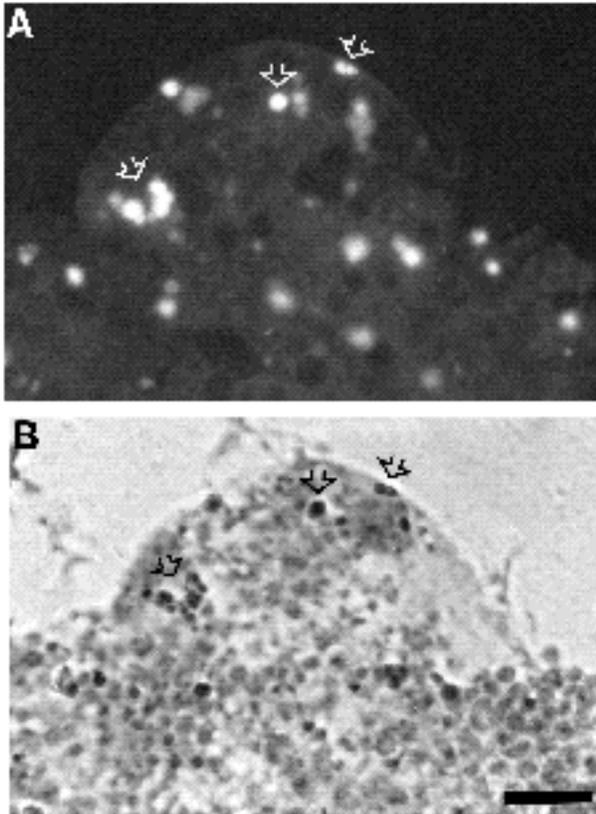
Fig. 4. Colocalization of acridine orange and toluidine blue in dissociated tissue. In order to assess the histogenetic properties of AO-positive cells, we examined preparations of tissue spreads before and after fixation (see methods). (A) A field of dissociated tissue from an AO-stained embryo prior to fixation. (B) The same field of tissue after fixation and subsequent toluidine blue staining (B). Arrows indicate several examples of in vivo AO-stained cells (white arrows) that also stain darkly with toluidine blue after fixation (black arrows). Scale bar, 75 µm.

for the occasional discrepancy between these staining procedures may include different dye affinity properties for cells at different stages of degeneration and/or losses of cells during the procedure. Nevertheless, these sequential comparisons established an excellent overall correspondence between cells that stained with AO in vivo and pyknotic cells that stained intensely with toluidine blue after fixation. Because toluidine-blue-stained figures are clearly apoptotic when examined by electron microscopy (see Fig. 2), these experiments establish that apoptotic cells in live *Drosophila* embryo are stained by the vital dyes AO and NB.

Vital dyes stain unengulfed and engulfed cell corpses

Our analyses of plastic sections and electron micrographs showed that many apoptotic cells were engulfed by macrophage-like cells. These phagocytes display an activity that is exceptionally similar to the scavenger-receptor mediated endocytosis found in mammalian macrophages (Abrams et al., 1992). To compare patterns of vital dye staining with the distribution of these engulfing cells, we

sought additional markers to visualize these phagocytes. For this purpose, we used an antibody against protein X, which labels vesicles and membranes of hemocytes in the *Drosophila* embryo. Immunolocalization studies and comparisons of cDNA sequences encoding protein X indicate that this protein is a product of hemocytes with functions characteristic of macrophages (Nelson, R. E., Fessler, L. I. and Fessler, J. H., unpublished data). When the distribution of this immunogen is compared to the AO-staining pattern of stage 13/14 embryos, a pattern of staining remarkably similar to the distribution of dying cells can be observed (Fig. 5, compare A with B). The coincidence between these staining patterns is particularly well illustrated at the leading edge of the dorsal epidermis during dorsal closure. This similarity persists during most embryonic stages with the notable exception of late stages in central nervous system development where prominent AO staining occurs in the absence of co-localizing hemocytes (not shown). Double-labelling experiments with anti-X antibody and toluidine blue demonstrate the presence of toluidine-blue-stained apoptotic bodies in many of the anti-X-positive cells (Fig. 5C-E). Note that only a portion of phagocytic cells that corresponds to the apoptotic corpses (see Fig. 2A,B) is stained by toluidine blue.

It was evident from our studies that AO and NB detect both free and phagocytosed cell corpses. Close examination of whole-mount and dissociated embryos stained in vivo shows small, individual, uniformly fluorescent cells representing unengulfed apoptotic bodies (small arrow in Fig. 6B). Free apoptotic corpses are the predominant, if not exclusive, form of staining in the maturing ventral nerve cord, as no phagocytosis of dead cells was observed in this tissue at this stage. Cell corpses that have already become engulfed can also be observed as discrete, vesicular staining inside phagocytes (Fig. 6A,C). Time-lapse studies show that AO staining of dead cell corpses can persist after engulfment for over 2 hours (data not shown). However, even in these advanced stages of cell death, the staining of these vital dyes is restricted to the engulfed cell corpses inside phagocytes. These experiments demonstrate that AO and NB, like toluidine blue, do not label macrophages directly. Phagocytes are only labelled when they contain one or more engulfed apoptotic corpses which are themselves selectively stained by these dyes. Finally, labelled corpses within macrophages are detected immediately upon staining of live embryos. Since the staining procedure takes only a few minutes, the majority, if not all, of the apoptotic corpses must have been engulfed prior to the AO treatment of embryos. We conclude that AO and NB are capable of staining apoptotic bodies after their engulfment and therefore must be able to readily enter and penetrate live phagocytes. These observations are relevant for the mechanism by which these vital dyes stain (see below and discussion).

Acridine orange staining is specific For apoptotic cell death

The mechanisms by which AO and NB stain degenerating cells are not known. In particular, it was not clear whether these vital dyes are general stains for dead cells, or whether they are selective for apoptosis. We explored this question
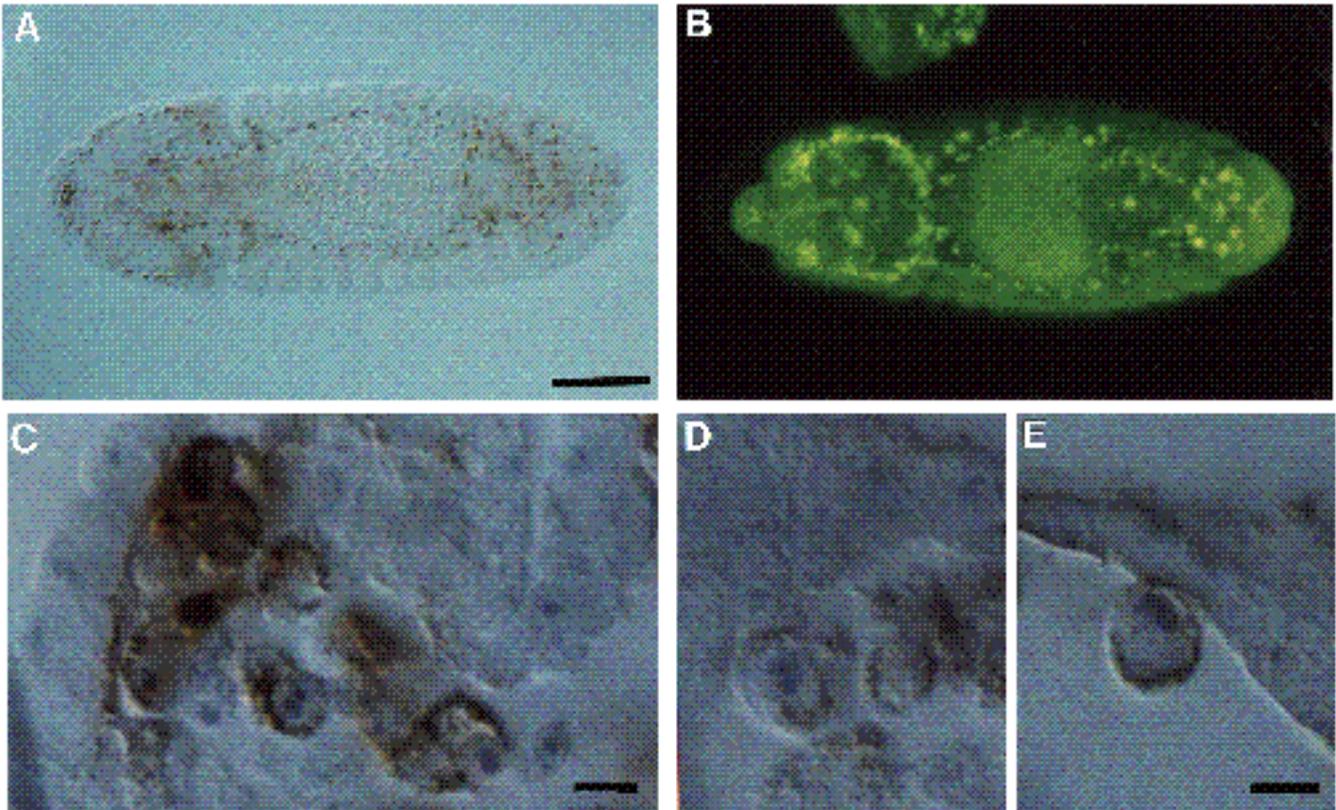
Fig. 5. Comparison of AO staining with the distribution of phagocytic hemocytes. (A) Dorsal view of a stage 14 embryo immunostained with anti-X antibody; scale bar, 50 µm. (B) Similarly aged embryo stained with AO; scale as in A, anterior is left. (C-E) High magnification views of toluidine-blue-stained plastic sections from anti-X-immunostained embryos. Note the presence of pyknotic, darkly stained material inside large, anti-X-positive cells. Scale bars in C and E, 10 µm.
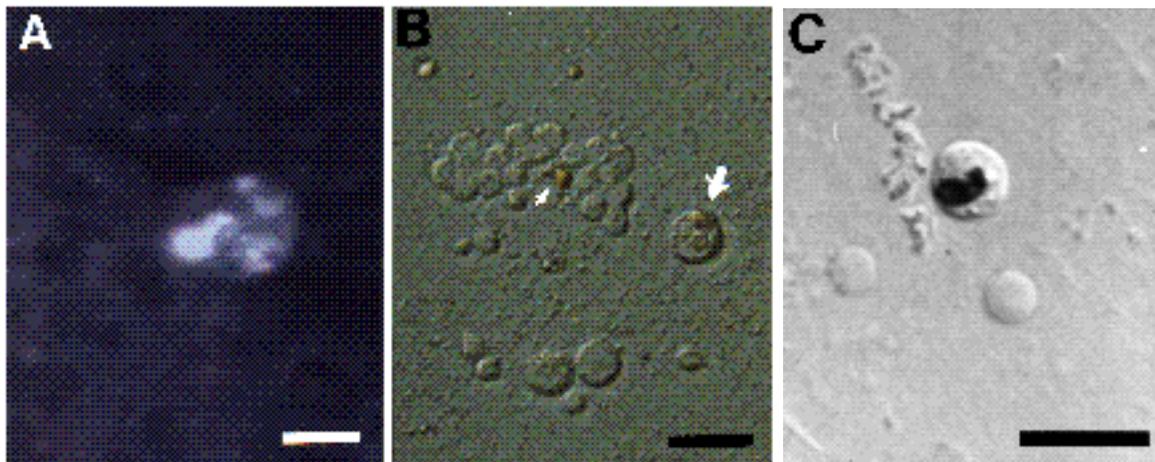

Fig. 6. Vital dyes stain cell corpses prior to and after engulfment. (A) Confocal image of a macrophage containing multiple AO-positive corpses in an AO-stained embryo; scale bar is 5 µm. (B) Nomarski optics of dissociated tissue from an AO-stained embryo. At this magnification, AO-positive material shows orange coloration without UV illumination. Note AO-positive unengulfed cell corpse (small arrow) and engulfed corpses (large arrow) which are also AO positive. Scale bar is 10 µm. (C) Nomarski optics of dissociated tissue from a nile-blue-stained embryo showing macrophage with engulfed nile-blue-positive corpses; scale bar, 10 µm.

by inducing an alternative form of cell death referred to as necrosis. Necrosis results from exposure to various external injuries, such as oxygen deprivation (hypoxia), abnormal temperature (hypo- and hyperthermia), or certain toxins (reviewed in Wyllie, 1981; Kerr and Harmon, 1991). Necrotic deaths are characterized by a general swelling of the cell, mitochondrial dilation, loss of membrane integrity and eventual plasma membrane rupture. This mode of death
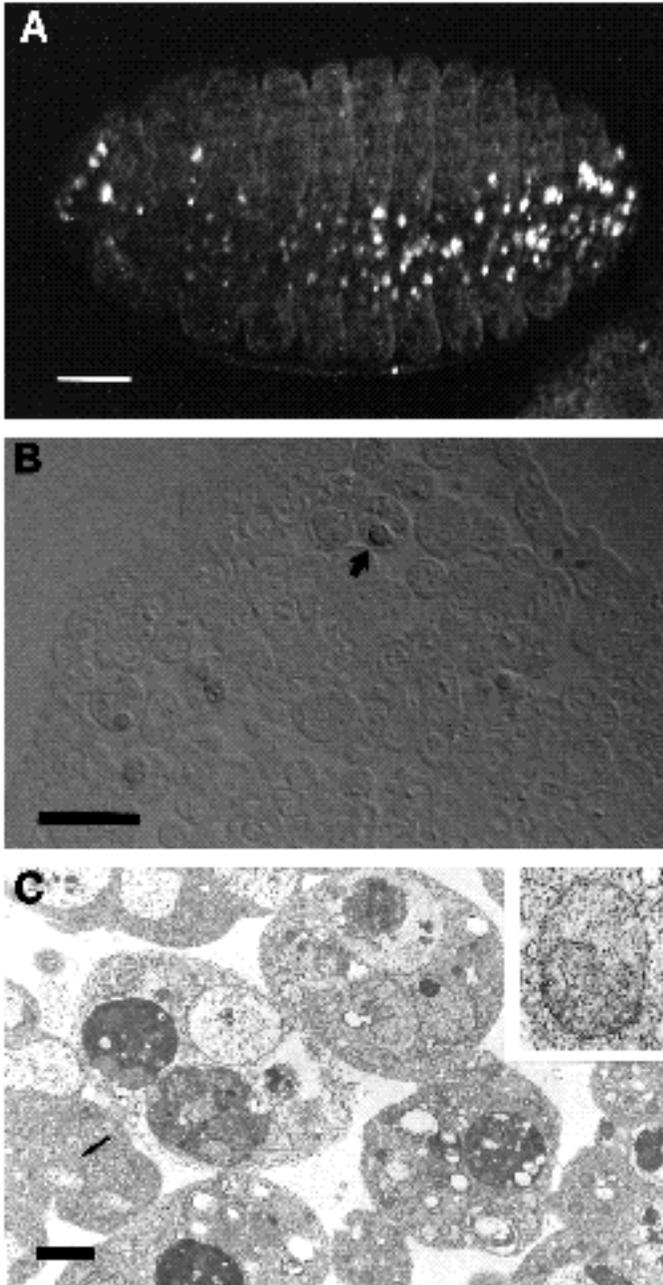
Fig. 7. Acridine orange does not detect necrotic cell death. (A) Embryo 10-12.5 hour AEL deprived of oxygen for 4 hours (see methods) and then stained with AO. This image is a superimposition of confocal optical sections collected in the red channel summed over a depth of ~30 μm. Note scattered AO-positive cells along the midline region; scale bar, 50 μm. (B) Toluidine-blue-stained plastic section of embryo (10-12 hour AEL) treated as in A. Arrow indicates macrophage containing at least one corpse; bar is 10 μm. (C) Electron micrograph from embryo (10-12 hour AEL) treated as in A. Arrow indicates swollen mitochondria indicative of necrotic death. Note extensive blebbing on the plasma membrane of the cell which is left of center. Several engulfed apoptotic cells are also visible. Inset shows typical mitochondrial morpholgy in these embryos. Scale bar, 2 μm, for inset the scale bar, 19 μm.

is dramatically distinct from apoptosis. To induce necrosis, *Drosophila* embryos were deprived of oxygen for a period of 4 hours (see methods) and then examined by electron microscopy. Cells from these embryos exhibit the characteristic features of necrosis including dilated mitochondria (Fig. 7C). When these embryos were stained with AO and observed in the green fluorescence channel (see Material and Methods), stage-specific staining of apoptotic cells was generally preserved, yet an enhanced level of background nuclear staining tended to obscure these images. Observations of AO staining in the red (rhodamine) channel showed no ectopic AO staining even though essentially every cell in these embryos suffered necrosis (Fig. 7A). Futhermore, embryos treated in this fashion retained the AO-staining pattern reminiscent of the staining observed at the developmental stage during which necrosis was induced (compare Fig. 7A to Fig. 9E). Similar results were obtained by staining plastic sections of these embryos with toluidine blue (Fig. 7B). Necrotic cells showed no significant increase in their affinity for toluidine blue, but the staining of apoptotic bodies was preserved.

AO staining in vivo and toluidine staining of plastic sections thus show parallel properties with respect to necrotic tissue. Necrotic cells are apparently not recognized by these dyes under the described conditions. We conclude that preferential staining with these dyes requires biochemical changes that are specific for apoptotic forms of death.

Analysis of ectopic cell death in embryonic mutants

We assessed the ability of vital dyes to detect ectopically induced cell death in mutants that perturb embryonic development. Mutations at *polyhomeotic* cause extensive degeneration in the ventral epidermis (Dura et al., 1987; Smouse and Perrimon, 1990). Embryos mutant for *polyhomeotic* exhibited excessive AO staining in this region and elsewhere (Fig. 8B). Mutations at *crumbs*, which cause massive degeneration of epithelial tissue (Tepass et al., 1990), also display ectopic AO staining that is widespread throughout the epidermis (Fig. 8C). Similar observations were obtained with NB (not shown).

We also induced cell death using X-irradiation which, in other systems, has been shown to cause protein synthesis-dependant apoptosis (see, for example, Umansky, 1991; Tomei, 1991). When 3-4 hour old wild-type embryos were exposed to a low dose of X-rays (600 rads), no staining was noted immediately after irradiation. However, after aging these embryos for 7 hours of physiological time, an excessive number of AO-positive cells was observed (Fig. 8D). Higher doses of X-irradiation (4000 rads) gave a more rapid and very noticeable increase of AO-labelled dying cells that displayed the ultrastructural features of apoptosis. In fact, AO-stained cells could be induced prior to the developmental stage at which the onset of cell death first appears. When 3-4 hour old embryos were irradiated at 4000 rads, aged for various times and then examined for AO staining, we found that dying cells were readily observed at least 2 hours earlier than would otherwise normally occur (see Fig. 8F). The appearance of precocious dying cells could be suppressed by cycloheximide treatments that immediately followed exposure to X-rays, sug-
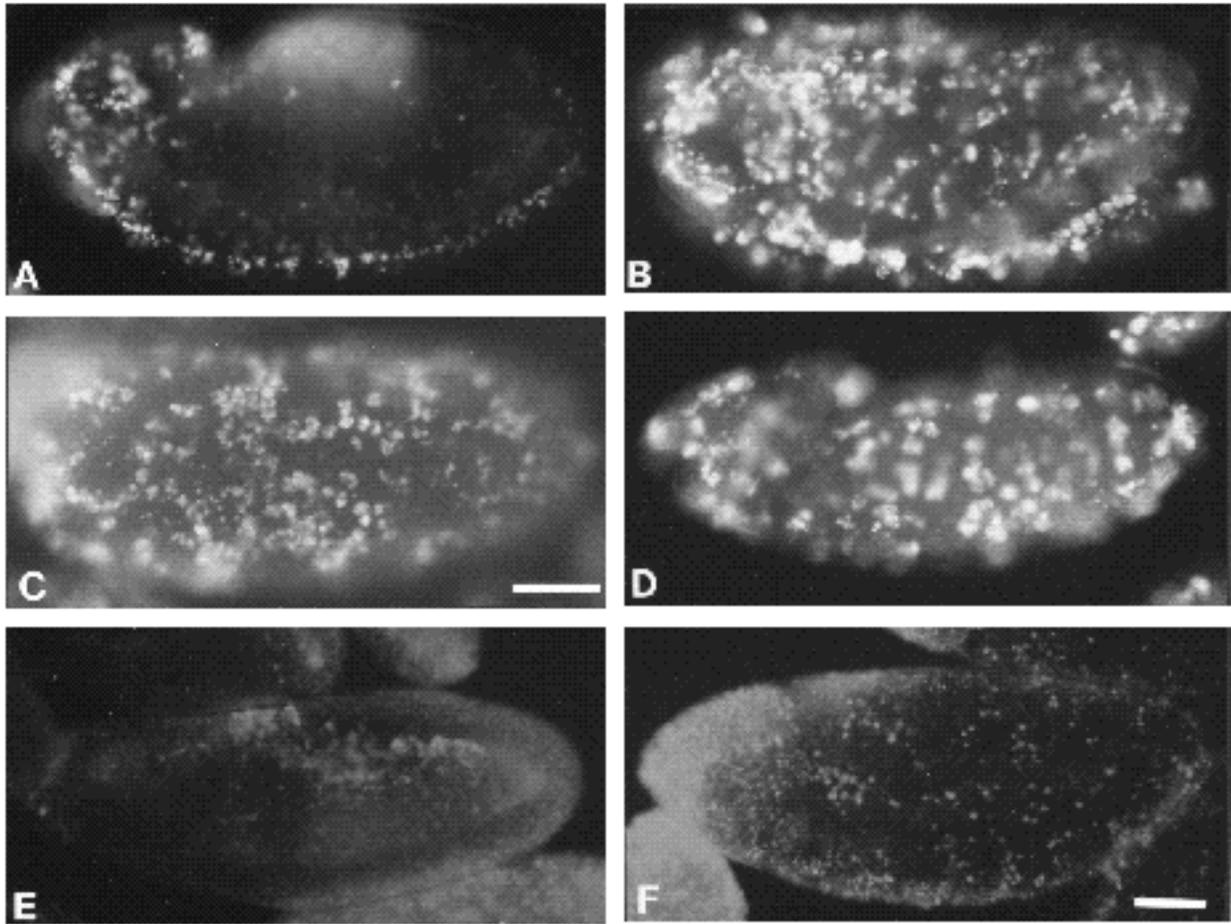
Fig. 8. Visualization of ectopic cell death by acridine orange and suppression of induced cell death by cycloheximide. Acridine-stained embryos in A, B and C are of comparable age. (A) Wild-type embryo, stage 13 (~10 hour AEL), (B) *polyhomeotic* mutant embryo (from an 8-11 hour AEL collection), (C) *crumbs* mutant embryo (from an 8-13 hour AEL collection), (D) X-irradiated embryo exposed to 600 rads at 3-4 hours AEL and then aged 14 hours at 18°C (see Methods). Embryos in E and F were exposed to 4000 rads X-irradiation and then aged 1.5 hours. Embryos in E were treated with cycloheximide immediately after irradiation whereas those in F received no such treatment (see Materials and Methods). Note that cycloheximide suppresses the appearance of acridine-positive cells. The brightly stained object in the lower right corner in E is an unfertilized egg which has considerable background fluorescence due to its high yolk content. Anterior is left, dorsal is up. Scale bars, 50 µm.

gesting that some aspect of irradiation-induced cell death is apparently dependent upon protein synthesis (Fig. 8E). These experiments serve to demonstrate the utility of the vital dyes AO and NB as tools to investigate the effect of mutations, environmental factors or chemical agents on programmed cell death in the *Drosophila* embryo.

Patterns of cell death during embryogenesis

Although the pattern of cell death during embryogenesis in *Drosophila* is quite dynamic, the overall distribution of dying cells is fairly reproducible for any given developmental stage. Prior to and during their ingestion by macrophages, dying cells are often extruded from a developing organ or cell layer (for example see Fig. 3). Because detection of cell death with vital dyes includes these late stages of degeneration, patterns observed with AO or NB reflect the position of dying cells as well as the accumulation of corpses in circulating phagocytes. Therefore, our observations do not necessarily reveal the precise original

position of a dying cell. However, since the pattern of cell death is very reproducible for a particular developmental stage, it appears that the original position of a dying cell typically approximates the final position of its corpse.

Since the following descriptive accounts of cell death are based on observations of embryos stained with AO and NB, it is important to keep in mind that these stains detect cell corpses that may have already fragmented into two or more apoptotic bodies. It is furthermore evident that one phagocyte may contain several stained corpses which might appear as a single stained structure (see Fig. 6). Finally, the continual disappearance of AO-stained cells with time allows only dynamic snapshots of cell death patterns, potentially leading to a significant underestimate of the total number of cell deaths. For these reasons, it is difficult to derive an accurate numerical estimate by this method. Nevertheless, to provide an impression of the scope of this process during embryogenesis, we occasionally cite num-
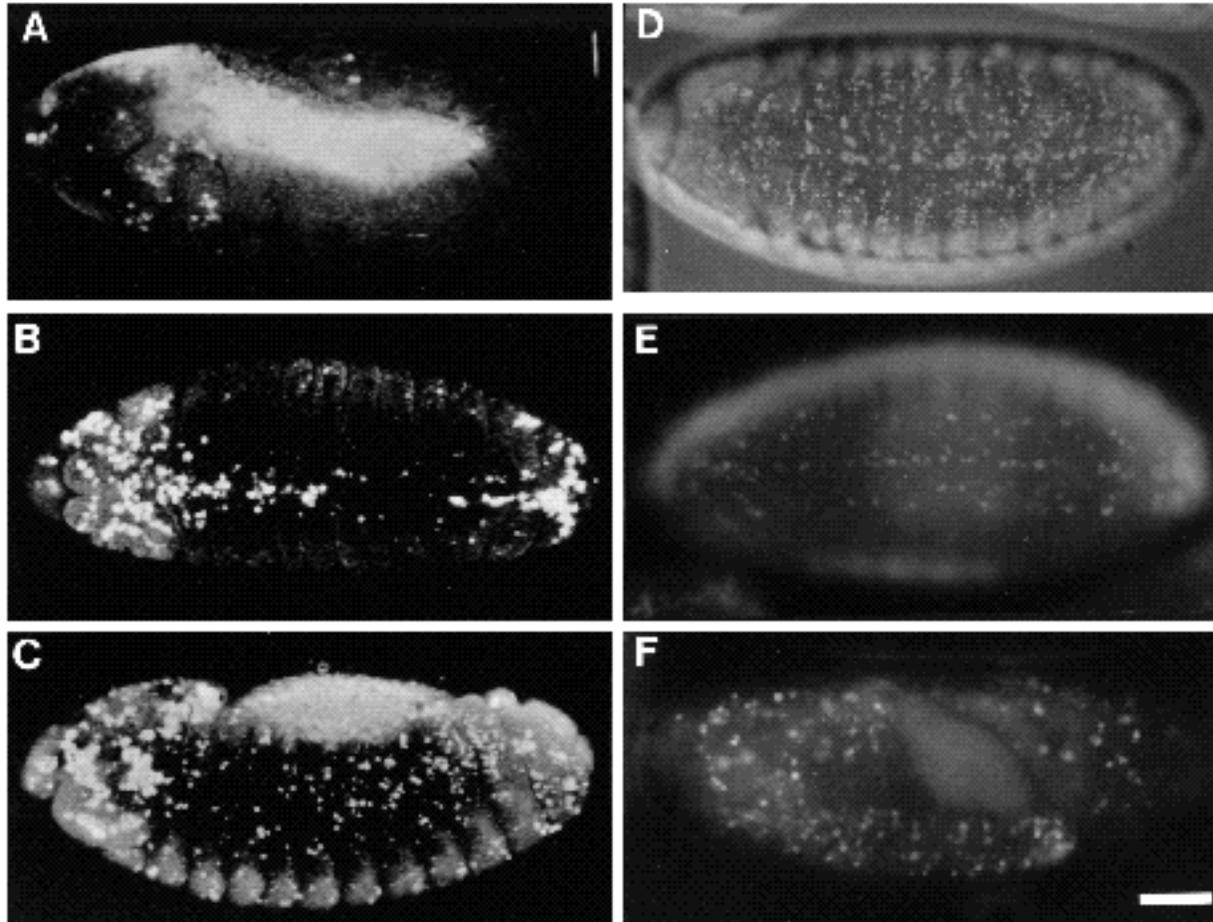
Fig. 9. Patterns of cell death during embryogenesis. AO-stained embryos viewed by graphic superimpositions of confocal optical sections (A-C) or fluorescence microscopy (D, double exposure of Nomarski and red channel, E, and F, green channel). Anterior is left. Note that yolk material throughout the center of the embryos gives diffuse, non-specific staining which is particularly prominent during earlier developmental stages. (A) Stage 12, lateral view. At this early stage, dying cells are found in the gnathal segments, the clypeolabrum and near the caudal tip of the retracting germ band. (B) Late stage 12, ventral view. Cell death spreads from both cephalic and caudal extremeties along the ventral midline axis. Prominent cell death in the ventral cephalic region is also found. (C) Stage 13, lateral view. Dying cells accumulate around the cephalic ganglia and beneath the dorsal ridge. Scattered deaths occur throughout the lateral epidermis. (D) Stage 13, ventral view. Segmentally reiterated deaths are found in the ventrolateral epidermis. (E) Stage 13/14, ventral view. One central and two lateral columns of cell deaths are apparent in the ventral portions of the embryo. (F) Late stage 16, lateral view. Note that prominent numbers of cells die in the central nervous system. Scale bar, 50 μm.

bers of AO-stained figures in the following descriptions. Because phagocytic cells do not circulate within the central nervous system, our quantitation of AO-stained figures in the ventral nerve cord are likely to represent a fairly accurate, stage-specific estimate of the number of cell deaths in this tissue.

Stage 11

We were unable to detect any signs of cell death until ~ 7 hours after egg laying (AEL) corresponding to the later part of the fully extended germ band stage. The first dying cells are invariably observed in the dorsal region of the head just anterior to the extended tip of the germ band. Apoptotic cells are also observed inside the epidermal cell layer of the gnathal segments and near the caudal tip of the extended germ band.

Stage 12

As the germ band retracts, stage 12, cell death becomes more widespread and prominent. During early germ band retraction, dying cells accumulate just beneath the developing epithelium of the gnathal segments, throughout the procephalic lobe region and within the interstitial space of the clypeolabrum (Fig. 9A). As the retracting germ band reaches 50% egg length, cell death becomes more prominent within the most posterior abdominal segments (Fig. 9A) and early signs of degeneration along the ventral midline can be observed within the most anterior thoracic segments. Cell death in the dorsal cephalic region, just beneath the dorsal ridge, also becomes very prominent (as in Fig. 9C). Scattered cell deaths also begin to appear in a segmentally reiterated pattern within the lateral portions of the ventral region (Fig. 9B). Toward the completion of germ band retraction, cell death is very conspicuous in the ven-

tral neurogenic region. It is interesting to note that the onset of cell death in this area does not occur simultaneously in all segments. Prominent numbers of dying cells first appear along the ventral midline in the thoracic and posterior abdominal segments yet they are nearly absent from mid-abdominal segments (Fig. 9B). Cell death within the mid-abdominal segments occurs on a slightly later schedule and, as germ band retraction proceeds, the waves of cell death along the midline eventually converge to form one continuous line (as in Fig. 9D).

Stage 13

With the exception of the central nervous system, all major zones of degeneration have been fully established by the completion of germ band retraction. By this stage (~ 9.5-10.5 hours AEL), cell death in the dorsal portion of the head becomes very prominent, as marked numbers of corpses accumulate around the supraoesophageal ganglia and beneath the dorsal ridge (Fig. 9C). Noticeable accumulation of corpses has also occurred within the clypeolabrum and just anterior of the salivary duct.

As this stage progresses, scattered and variable numbers of cell deaths are evident throughout the epidermis of the embryo (Fig. 9C). Within the dorsolateral portion of each hemisegment, for example, 15 to 50 AO-stained figures are typically observed at any given point during this stage. Segmentally reiterated AO staining in the ventrolateral portions of the epidermis is also very prominent (Fig. 9D). Clusters of AO-positive cells accumulate along the midline (Fig. 9B,D), which are clearly associated with phagocytic macrophages (not shown). Lateral to the midline, up to 30 AO-positive figures appear at a slightly later point in stage 13 and are scattered throughout the most ventral portion of each hemisegment (compare Fig. 9D with B). The vast majority of dying cells in this region accumulate in the interstitial spaces between the ventral epidermis and the nerve cord. We have thus far been unable to determine whether these corpses originated from cells that were committed to neural or epidermal fates. By the end of this stage, the pattern of cell death in the ventrolateral region gradually evolves into one central and two lateral columns of macrophage associated staining along this portion of the embryo (Fig. 9E). The position of cells in the central, midline column is fairly consistent among the segments whereas the lateral columns, although also segmented in character, tend to show more variably positioned cell death figures.

Stage 14

The AO- and NB-staining cells generally tend to persist from the previous stages, especially along the ventral midline and in the head region. As this stage progresses (~10.5-11.5 hours AEL), a new and continuous ring of dying cells becomes evident at the leading edge of the dorsally closing tissue during gut closure (see Fig. 5B). At this stage, degenerating cells are rapidly phagocytosed by neighboring macrophages (see Fig. 5).

Stage 15

Once dorsal closure is complete (~13 hours AEL), the general domains of vital dye staining from earlier stages fade
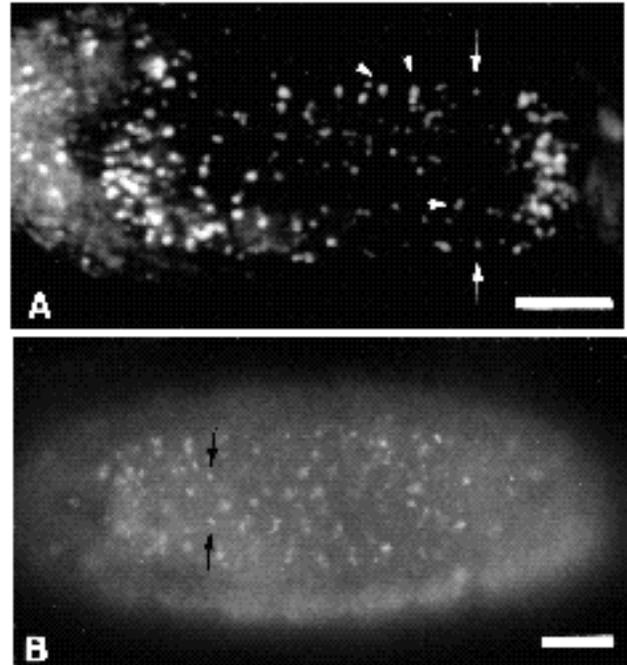

Fig. 10. Cell death in the embryonic central nervous system. Stage 16 embryos were stained with AO and the ventral nerve cord was viewed by graphic summation of confocal optical sections (A) or fluorescence microscopy (B). Close examination of AO staining on either side of the midline axis reveals symmetric and asymmetric patterns of cell death in this tissue. Examples of symmetric deaths are denoted by full arrow pairs and several examples of asymmetric cell deaths are denoted by arrowheads. Anterior is left. Scale bars, 50 µm.

and sporadic cell deaths occur throughout the body cavity (not shown). Many of these dying cells are localized just inside of the body wall or around the mid-gut. The appearance and position of this staining pattern suggests an association with phagocytic macrophages. Toward the end of this stage, cell death begins to occur in the condensing central nervous system.

Stage 16

As the nerve cord condenses (~14 hours AEL), large numbers of cell deaths can be observed with vital dyes throughout the central nervous system (note staining within the brain and the ventral nerve cord in Fig. 9F). At this stage, neuromuscular development matures to the extent that twitching movements can be observed. Phagocytic hemocytes do not invade the tightly packed cell body layer of the central nervous system (CNS) and, hence, unlike cell deaths in other regions, no engulfment by circulating macrophages occurs in this region. The pattern of vital dye staining in the CNS should therefore most accurately reflect the precise position and numbers of apoptotic cells. We analyzed AO staining within the ventral nerve cord by superimposing optical sections that extend through this portion of the CNS. These analyses result in a graphic summation of cell death through the entire depth of the ventral cord (Fig. 10A). Using this technique in combination with time-lapse preparations (see Methods), we have followed many

AO-positive cells in the CNS for up to 45 minutes. Fig. 10A shows one such example of cell death in a condensed ventral nerve cord where most of the AO-stained cells are positioned at the anterior and posterior termini. Approximately 140 AO-positive cells were detected at this stage. At a slightly earlier stage, cell death is more uniformly distributed over the length of the ventral cord and appears segmentally reiterated (Fig. 10B). A similar pattern of degeneration has been reported during late embryogenesis in the CNS of *Calliphora* (Starre-van der Molen and Otten, 1974).

Comparative analyses of AO staining on either side of the midline reveals an overall symmetry in the pattern of cell deaths in the condensing ventral nerve cord (Fig. 10A,B). Although the precise number and position of AO-stained cells may vary, cell death on one side of the ventral midline is often accompanied by a similarly positioned dying cell(s) on the opposite side of the midline. There are, however, clear instances of asymmetric cell deaths in the nervous system as well. These asymmetries are more readily observed at later stages of ventral nerve cord maturation when neural cell death is somewhat less prominent. As shown in Fig. 10A, AO-positive cells are not always accompanied by a similarly positioned dying cell(s) on the opposite side of the midline. Because AO staining can persist for relatively long periods in these preparations (at least 45 minutes), sporadic variances of a temporal nature are unlikely to be the entire cause for asymmetric staining. We suggest that asymmetric cell deaths in the nerve cord may reflect some degree of plasticity in the control of cell death during embryonic CNS development (see Discussion).

Summary of cell death during *Drosophila* embryogenesis

The earliest appearance of cell death is observed in the dorsal cephalic region, within the gnathal segments and in the clypeolabrum as the germ band begins to retract (stage 11). Thereafter, as germ band retraction proceeds (stages 12 and 13), cell death becomes widespread throughout the embryo, particularly in the ventrolateral portions and around the procephalic lobes. Large numbers of degenerating cells accumulate in the interstitial spaces beneath the dorsal ridge, along the ventral midline and within the gnathal segments. During dorsal closure, a zone of degenerating cells, organized in the shape of a ring, forms around the closing dorsal tissue (stage 14). As head involution becomes well advanced (stage 15), zones of vital dye staining from earlier stages subside and scattered subepidermal staining appears throughout the embryo. Eventually, prominent cell death appears throughout the CNS as the ventral nerve cord condenses (stage 16). In contrast to earlier stages, cell death in the cell body layer of the ventral cord and brain hemispheres at this time is not associated with phagocytic macrophages.

DISCUSSION

The deliberate and orderly removal of cells by naturally occurring cell death is an integral part of animal development. Despite the importance of this regressive process during normal development and in pathological situations, much remains to be learned about the underlying molecular mechanisms. We believe that dramatic progress can be made in this area by taking advantage of the powerful genetic and molecular techniques available in *Drosophila*. In this paper, we examined the general features and distribution of programmed cell death in wild-type embryos to establish the foundation for further molecular genetic studies.

The results from our ultrastructural analysis indicate that cell death in the *Drosophila* embryo occurs by apoptosis. We found that embryonic cell deaths involve separation from neighboring cells, nuclear condensation, cytoplasmic shrinkage, fragmentation and engulfment by circulating macrophages. These cytological changes closely parallel the features of apoptotic cell death described in other systems (for examples see Wyllie, 1981; Kerr and Harmon, 1991). Degenerate ovarian chambers in adult *Drosophila* females also show ultrastructural features that resemble apoptotic cell death (Giorgi and Deri, 1976). Similarly, the eye disc of wild-type or mutant larvae contain cells that appear apoptotic (Fristrom, 1969, Wolff and Ready, 1991). However, Wolff and Ready (1991) noted an absence of marginal condensation from the nuclear membrane during cell death in the eye disc and also reported that, subsequent to cellular fragmentation, the nuclei within subcellular bodies can assume necrotic-like features. Because our ultrastructural studies show little indication of necrosis in embryonic tissue, we suspect that variations in the final mode of structural collapse may arise from tissue-specific differences (Clarke, 1990).

In order to visualize cell death rapidly and reliably in the *Drosophila* embryo, we adopted vital dye staining techniques that were originally developed for the analysis of imaginal tissues (Spreij, 1971). We find that acridine orange (AO) and nile blue (NB) stain individual apoptotic cells, both prior to and after engulfment, but not macrophages per se. Because of the ease and speed of these assays, it should be possible to study the effect of rather large numbers of mutations or chemical compounds on apoptosis. The mode by which these dyes preferentially stain dead cells is not known, although several possible mechanisms, including increased membrane permeability, seem plausible. However, we find that apoptotic corpses inside macrophages are clearly labelled. Therefore, these dyes must be able to enter and penetrate live cells readily. Furthermore, cells undergoing necrotic death induced by hypoxia were not stained by AO (as visualized in the red channel). These observations indicate that AO can be used to visualize selectively apoptotic forms of death, and that selective staining by AO is not merely a passive consequence resulting from compromised membrane permeability (for a review of the cytochemical properties of AO, see Kasten, 1967). Likewise, toluidine blue staining of fixed tissue sections resulted in highly specific labelling of apoptotic forms of death, leaving necrotic cells completely unstained. We conclude that biochemical changes characteristic for apoptotic forms of death are responsible for the selective affinity to AO and toluidine blue.

Many corpses resulting from programmed cell death are avidly engulfed by circulating macrophage-like cells in the

Drosophila embryo (see also Campos-Ortega and Hartenstein, 1985). The characteristic phagocytic activity associated with these cells is further emphasized by the observation that they express an endocytic receptor activity (Abrams et al., 1992) which is remarkably similar to the scavenger receptor activity found in mammalian macrophages (Goldstein et al., 1979, Kodama et al., 1990). In addition, circulating phagocytes synthesize a number of basement membrane components during embryogenesis (Fessler and Fessler, 1989). Macrophage-like cells are thus involved with multiple histogenetic functions during this stage of *Drosophila* development.

We used vital dye staining to catalogue the pattern of cell death throughout embryogenesis in *Drosophila*. Although the distribution of dying cells changes dramatically during development, the pattern of cell death for any given developmental stage was remarkably reproducible. Therefore, the induction of these deaths appears to be tightly controlled and must result from 'natural causes'. It is apparent from our studies that a large number of cells die at many different times and in many different tissues and regions of the embryo. Our methods of imaging cell death, however, do not readily allow for a precise census of the number of cell deaths in most contexts. There are several limitations to the use of AO and NB as a means to count cell deaths. First, dying cells can fragment into multiple AO-stained apoptotic bodies. Second, most of the dying cells are rapidly engulfed by phagocytes. A single phagocyte usually contains multiple cell corpses, which are labelled by AO and NB, but may appear as a single stained structure. Finally, the continual loss of cells that were 'pulse-stained' over time means that these methods provide only a static snap-shot image of a very dynamic process. Nevertheless, for reasons discussed below, we feel that a reasonable numerical assessment of cell deaths can be made in the ventral nerve cord. Assuming that there are approximately 300 cells in each segment at this stage (Poulson, 1950; Truman and Bate, 1988), we estimate that at least 4% of this neural population undergoes programmed cell death. Because our counts derive from static rather than cumulative images, we feel that this represents a very conservative estimate.

Even though bilateral symmetry of cellular age and identity is generally well preserved throughout the *Drosophila* central nervous system (for example Campos-Ortega and Hartenstein, 1985; Doe et al., 1988; Klämbt et al., 1991), clear asymmetries in the exact number and position of cell deaths on either side of the ventral cord midline were found. These differences are significant because they are not easily explained either by subtle temporal variances, or by relocation of dead cells upon phagocytosis in migratory cells. First, time-lapse studies demonstrate that apoptotic cells in the CNS retain AO staining for at least 45 minutes, arguing strongly against small sporadic temporal differences as a potential explanation for our observations. Second, based on electron microscopy and Anti-X staining, we know that circulating macrophages do not have access to degenerating cells within the CNS cell body layer. In this context, a dying cell is unlikely to wander far from its original position. Therefore, it appears that the onset of cell deaths in the CNS is at least somewhat variable. Although we cannot entirely rule out positional or temporal variances as explanations for the asymmetries in the pattern of cell deaths, it is possible that some apoptotic deaths are not strictly predetermined during the later stages of CNS development in the *Drosophila* embryo. Plasticity in the control of cell deaths has been well documented during postembryonic development (e.g. Kimura and Truman, 1990, Fischbach and Technau, 1984, Steller et al., 1987, Wolff and Ready, 1990; Campos et al., 1992). Similar interactive processes may regulate cell survival during embryogenesis. Many mutants affecting embryonic (see, for example Dura et al., 1987; Magrassi and Lawrence,1988; Tepass et al., 1990) or imaginal development (Fristrom, 1969; James and Bryant, 1981; Bonini et al., 1990) show ectopic death. Moreover, cell death in *ftz* mutants is not restricted to cells that would normally express this gene product (Magrassi and Lawrence, 1988). Hence, as is the case for many organisms, *Drosophila* also displays a capacity to eliminate cells that do not successfully complete their developmental program.

In a variety contexts, it has been shown that cell death is an active process which can be blocked or delayed by inhibitors of protein synthesis (Tata, 1966; Lockshin, 1969; Farbach and Truman, 1988; Martin et al., 1988; Oppenheim et al., 1990). We explored this issue in the *Drosophila* embryo with the use of cycloheximide. Although very early treatments with this agent prevented the appearance of AO-stained cells, it was also clear that these treatments had imposed such general and widespread effects upon development that a meaningful assessment of the result was impossible. In contrast, when cycloheximide was introduced at a later stage, shortly before the first onset of cell deaths, their occurrence was not affected. However, we did find that X-irradiation-induced cell deaths could be suppressed by cycloheximide treatment. These precocious cell deaths apparently depend upon some aspect of de novo protein synthesis. More direct evidence for the active nature of cell death in *Drosophila* comes from the identification of mutations that block all embryonic cell deaths (White, K., Abrams, J. M., Grether, M., Young, L. and Steller, H., unpublished data, see below).

The work described in this paper provides the basis for the isolation of cell death defective mutants in *Drosophila*. Genes required for distinct steps in a cell death pathway (eg. specification, execution, engulfment and degradation) have already been identified in the nematode *C. elegans* (reviewed in Ellis et al., 1991). Comparative analyses of these loci with genetic components identified in *Drosophila* may elucidate some aspects of the cell death pathway that have been conserved between these evolutionarily disparate organisms. In contrast to the situation in *C. elegans* (Sulston and Horvitz, 1977; Ellis et al., 1991), at least some programmed cell in *Drosophila* are not strictly predetermined by lineage. For example, some postembryonic cell deaths require hormone induction (Kimura and Truman, 1990) and the survival of certain cells in the visual system depends on cellular interactions (see for example Fischbach and Technau, 1984; Wolff and Ready, 1990, Campos et al., 1992). This plasticity offers a unique opportunity to study how cell interactions may lead to the specification of the cell death fate.

We have recently completed a screen for cell death defective mutations and have identified one locus that is required for virtually all programmed cell deaths that occur during *Drosophila* embryogenesis (White, K., Abrams, J. M., Grether, M., Young, L. and Steller, H., unpublished data). We expect that the biochemical characterization of this locus and further genetic studies in *Drosophila* will contribute significantly to a better understanding of the molecular mechanisms underlying programmed cell death.

REFERENCES

Abrams, J., Lux, A., Steller, H., and Krieger, M. (1992). Macrophages in *Drosophila* embryos and L2 cells exhibit scavenger receptor-mediated endocytosis. *Proc. Natl. Acad. Sci. USA* **89**, 10375-10379.

Bonini, N. Leiserson, W. and Benzer, S. (1990). A mutation in compound eye development of Drosophila that results in cell death rather than differentiation. *J. Cell. Biochem.* **14E**, 502.

Bowen, I. D. and Lockshin, R. A. (1981). *Cell Death in Biology and Pathology.* London: Chapman and Hall.

Bowen, I. D. (1981). Techniques for demonstrating cell death. In *Cell Death in Biology and Pathology.* (ed. I. D. Bowen and R. A. Lockshin) pp. 381-444. London: Chapman and Hall.

Cagan, R. L. and Ready, D. F. (1989). *Notch* is required for successive cell decisions in the developing Drosophila retina. *Genes Dev.* **3**, 1099-1112.

Campos, A. R., Fischbach, K. F. and Steller, H. (1992). Survival of photoreceptor neurons in the compound eye of *Drosophila* depends on connections with the optic ganglia. *Development* **114**, 355-366.

Campos-Ortega, J. A. and Hartenstein, V. (1985). *The Embryonic Development of* Drosophila melanogaster. Berlin: Springer-Verlag.

Clarke, P. G. H. (1990). Developmental cell death: morphological diversity and multiple mechanisms. *Anat. Embryol.* **181**, 195-213.

Doe, C. Q., Hiromi, Y. Gehring, W. J. Goodman, C. S. (1988). Expression and function of the segmentation gene *fushi tarazu* during *Drosophila* neurogenesis. *Science* **239**, 170-175.

Dura, J., Randsholt, N. B., Deatrick, J., Erk, I., Santamaria, P., Freman, J. D., Freeman, S. J., Weddell, D. and Brock, H. W. (1987). A complex genetic locus, *polyhomeotic*, is required for segmental specification and epidermal development in D. melanogaster. *Cell* **51**, 829-839.

Echalier, G. (1976). *In vitro* established lines of *Drosophila* cells and applications in physiological genetics. In *Invertebrate Cell Culture. Applications in Medicine, Biology and Agriculture* (ed. E. Kurstak and K. Maramorosch), pp 131-150. New York: Academic Press.

Ellis, H. M. and Horvitz, H. R. (1986). Genetic control of programmed cell death in *C. elegans. Cell* **44**, 817-829.

Ellis, R. E., Yuan, J. and Horvitz, H. R. (1991). Mechanisms and fuctions of cell death. *Annu. Rev. Cell. Biol.* **7**, 663-698.

Fessler, J. H. and Fessler, L. I. (1989). *Drosophila* extracellular matrix. *Ann Rev. Cell. Biol.* **5**, 309-339.

Farbach. S. E. and Truman, J. W. (1988). Cycloheximide inhibits ecdysteroid-regulated neuronal death in the moth *Manduca sexta. Society Neurosci. Abst.* **14**, 368.

Fischbach, K. F. and Technau, G. (1984). Cell degeneration in the developing optic lobes of the sine oculis and small-optic-lobes mutants of *Drosophila melanogaster. Dev. Biol.* **104**, 219-239.

Fristrom, D. (1969). Cellular degeneration in the production of some mutant phenotypes in *Drosophila melanogaster. Molec. Gen. Genetics* **103**, 363-379.

Giorgi, F, and Deri, P. (1976). Cell death in the ovarian chanmbers of *Drosophila melanogaster. J. Embryol. Exp. Morph.* **35**, 521-533.

Goldstein, J. L., Ho, Y. K., Basu S. K., and Brown, M. (1979). Binding site on macrophages that mediates uptake and degradation of acetylated low density lipoprotein, producing massive cholesterol deposition. *Proc. Natl. Acad. Sci. USA* **76**, 333-337.

Hedgecock, E. M., Sulston, J. E. and Thomson, J. N. (1983). Mutations affecting programmed cell deaths in the nematode *Caenorhabditis elegans. Science* **220**, 1277-1279.

Hengartner, M. O., Ellis, R. E. and Horvitz, H. R. (1992). *Caenorhabditis elegans* gene *ced*-9 protects cells from programmed cell death. *Nature* **356**, 494-499.

Hinchcliffe, J. R. (1981). Cell death during embryogenesis. In *Cell Death in Biology and Pathology.* (ed. I. D. Bowen and R. A. Lockshin) pp. 35-78. London: Chapman and Hall.

Hurle, J. M. (1988). Cell death in developing systems. *Meth Achiev. Exp. Pathol.* **13**, 55-86.

James, A. A. and Bryant, P.J. (1981). Mutations causing pattern deficiencies and duplications in the imaginal wing disk of *Drosophila melanogaster. Dev. Biol.* **85**, 39-54.

Kasten, F. H. (1967). Cytochemical studies with acridine orange and the influence of dye contaminants in the staining of nucleic acids. In *Interantional Review of Cytology,* vol. 21 (ed. G. H. Bourne and J. F. Danielli) pp.141-202. New York: Academic Press.

Kerr, J. F. R., Wyllie, A. H. and Currie, A. R. (1972). Apoptosis: a basic biological phenomenon with wide ranging implications in tissue kinetics. *Br. J. Cancer.* **26**, 239-257.

Kerr, J. F. R. and Harmon, B. V. (1991). Definition and incidence of apoptosis: an historical perspective. In *Apoptosis: the Molecular Basis of Cell Death* (eds. L. D. Tomei and F. O. Cope) pp. 5-29. New York: Cold Spring Harbor Laboratory Press.

Kimura, K. and Truman, J. W. (1990). Postmetamorphic cell death in the nervous and muscular systems of *Drosophila melanogaster. J. Neurosci.* **10**, 403-411.

Klämbt, C, Jacobs, R. J. and Goodman, C. S. (1991). The midline of the Drosophila central nervous sytem: A model for the genetic analysis of cell fate, cell migration, and growth cone guidance. *Cell* **64**, 801-815.

Kodama, T., Freeman, M., Rohrer, L., Zabrecky, J., Matsudaira, P. and Kreiger, M. (1990). Type I macrophage scavenger receptor contains alpha-helical and collagen-like coiled coils. *Nature* **343**, 531-535.

Lee, K. J., Freeman, M. and Steller, M. (1991). Expression of the *disconnected* gene during development of *Drosophila melanogaster. EMBO J.* **10**, 817-826.

Lockshin, R. A. (1969). Programmed cell death. Activation of lysis by a mechanism involving the sythesis of protein. *J. Insect Physiol.* **15**, 1505-1516.

Lockshin, R. A. and Zakeri, Z. (1991). Programmed cell death and apoptosis. In *Apoptosis: the Molecular Basis of Cell Death* (eds. L. D. Tomei and F. O. Cope), pp. 47-60. New York: Cold Spring Harbor Laboratory Press.

Martin, D. P., Schmidt, R. E., DiStefano, P. S., Lowry, O. H., Carter J. G. and Johnson, E. M. (1988). Inhibitors of protein synthesis and RNA synthesis prevent neuronal death caused by nerve growth factor deprivation. *J. Cell Biol.* **106**, 829-844.

Magrassi, L. and Lawrence, P. A. (1988). The pattern of cell death in *fushi tarazu*, a segmentation gene of *Drosophila. Development* **104**, 447-451.

Murphy, C. (1974). Cell death and autonomous gene action in lethals affecting imaginal discs in *Drosophila melanogaster. Dev. Biol.* **39** 23-36.

Olson, P. F., Fessler, L. I., Nelson, R. E., Sterne, R. E., Campbell, A. G., and Fessler, J. H. (1990). Glutactin, a novel *Drosophila* basement membrane-related glycoprotein with sequence similarity to serine esterases. *EMBO J.* **9**, 1219-1227.

Oppenheim, R. W. (1985). Naturally occurring cell death during neural development. *Trends Neurosci.* **8**, 487-493.

Oppenheim, R. W., Prevette, D., Tytell, M., and Homma, S. (1990). Naturally occurring and induced neuronal cell death in the chick embryo *in vivo* requires protein and RNA synthesis: evidence for the role of cell death genes. *Dev. Biol.* **138**, 104-113.

Osborne, M. P. (1980). Electron-microscopic methods for nervous tissues. In *Neuroanatomical Techniques: Insect Nervous System* (eds. N. J. Strausfield and T. A. Miller), pp. 231-235. New York: Springer-Verlag.

Poulson, D. F. (1950). Histogenesis, organogenesis, and differentiation in the embryo of *Drosophila melanogaster* Meigen. In *Biology of Drosophila* (ed. M. Demerec) pp. 168-264. New York: Wiley.

Raff, M. C. (1992). Social controls on survival and cell death. *Nature* **356**, 397-400.

Robbins, E. and Marcus, P. I. (1963). Dynamics of acridine-orange cell interaction. *J. Cell Biol.* **18**, 237-250.

Savill, J., Dransfield, I., Hogg, N. and Haslett, C. (1990). Vitronectin receptor-mediated phagocytosis of cells undergoing apoptosis. *Nature* **343**, 170-173.

Saunders, J. W., Gasseling, M.T. and Saunders, L. C. (1962). Cellular death in morphogenesis of the avian wing. *Dev. Biol.* **5**, 147-178.

Saunders, J. W. (1966). Death in embryonic sytems. *Science* **154**, 604-612.

Smouse, D. and Perrimon, N. (1990). Genetic dissection of a complex neurological mutant, polyhomeotic, in *Drosophila. Dev. Biol.* **139**, 169-185.

Spreij, T. E. (1971). Cell death during the development of the imaginal discs of Calliphora erythrocephala. *Netherlands J. Zool.* **21**, 221-264.

Spurr, A. R. (1969). A low viscosity epoxy resin embedding medium for electron microscopy. J. *Ultrastruct. Res.* **26**, 31-43.

Starre-van der Molen, L. G. and Otten, L. (1974). Embryogenesis of *Calliphora erythrocephela* Meigen. Cell death in the central nervous system during late embryogenesis. *Cell Tissue Res.* **151**, 219-228.

Steller, H., Fischbach, K. F. and Rubin, G. M. (1987). *disconnected*: a locus required for neuronal pathway formation in the visual system of *Drosophila. Cell* **50**, 1139-1153.

Sulston, J. E. and Horvitz, H. R. (1977). Postembryonic cell lineages of the nematode *Caenorhabditis elegans. Dev. Biol.* **56**, 110-156.

Tata, J. R. (1966). Requirement for RNA and protein synthesis for induced regression of tadpole tail in organ culture. *Dev. Biol.* **13**, 77-94.

Tepass, U., Theres, C. and Knust, E. (1990). *crumbs* encodes an EGF-like protein expressed on apical membranes of Drosophila epithelial cells and required for organization of epithelia. *Cell* **61**, 787-799.

Tomei, L. D. (1991). Apoptosis: A program for death or survival? In *Apoptosis: the Molecular Basis of Cell Death* (eds. L. D. Tomei and F. O. Cope) pp. 279-316. New York: Cold Spring Harbor Laboratory Press.

Tomei, L. D. and Cope, F. O. (1991). *Apoptosis: the Molecular Basis of Cell Death.* New York:Cold Spring Harbor Laboratory Press.

Truman, J. W. (1984). Cell death in invertebrate nervous sytems. *Ann. Rev. of Neurosci.* **7**, 171-188.

Truman, J. W. and Bate, M. (1988). Spatial and temporal patterns of neurogenesis in the central nervous sytem of *Drosophila melanogaster*. *Dev. Biol.* **125**, 145-157.

Trump, B. F., Berezesky, I. K. and Osornio-Vargas, A. R. (1981). Cell death and the disease process. The role of calcium. In *Cell Death in Biology and Pathology* (eds. I. D. Bowen and R. A. Lockshin), pp. 209-242. London: Chapman and Hall.

Umansky, S. R. (1991). Apoptotic process in the radiation-induced death of lymphocytes. In *Apoptosis: the Molecular Basis of Cell Death* (eds. L. D. Tomei and F. O. Cope) pp.193-208. New York: Cold Spring Harbor Laboratory Press.

Whitten, J. M. (1969). Cell death during early morphogenesis: Parallels between Insect limb and vertebrate limb development. *Science* **163**, 1456-1457.

Wolff, T. and Ready, D. F. (1991). Cell death in normal and rough eye mutants of *Drosophila*. *Dev. Biol.* **113**, 825-839.

Wyllie, A. H., Kerr, J. F. R. and Currie A. R. (1980). Cell death: the significance of apoptosis. *Int. Rev. Cytol.* **68**, 251-306.

Wyllie, A. H. (1980). Glucocorticoid-induced thymocyte apoptosis is associated with endogenous endonuclease activation. *Nature* **284**, 555-557.

Wyllie, A. H. (1981). Cell death: a new classification separating apoptosis from necrosis. In *Cell Death in Biology and Pathology* (eds. I. D. Bowen and R. A. Lockshin), pp 9-34. London: Chapman and Hall.

Yuan, J. and Horvitz, H. R. (1990). The *Caenorhabditis elegans* genes ced-3 and ced-4 act cell autonomously to cause programmed cell death. *Dev. Biol.* **138**, 33-41.